NASA/TM–20230003195

Protective Coatings for Lunar Dust Tolerance

Valerie. L. Wiesner, Christopher J. Wohl, Glen C. King and Keith L. Gordon
Langley Research Center, Hampton, Virginia

Lopamudra Das and Jonathan J. Hernandez
National Institute of Aerospace, Hampton, Virginia

April 2023

NASA STI Program . . . in Profile

Since its founding, NASA has been dedicated to the advancement of aeronautics and space science. The NASA scientific and technical information (STI) program plays a key part in helping NASA maintain this important role.

The NASA STI program operates under the auspices of the Agency Chief Information Officer. It collects, organizes, provides for archiving, and disseminates NASA's STI. The NASA STI program provides access to the NTRS Registered and its public interface, the NASA Technical Reports Server, thus providing one of the largest collections of aeronautical and space science STI in the world. Results are published in both non-NASA channels and by NASA in the NASA STI Report Series, which includes the following report types:

- TECHNICAL PUBLICATION. Reports of completed research or a major significant phase of research that present the results of NASA Programs and include extensive data or theoretical analysis. Includes compilations of significant scientific and technical data and information deemed to be of continuing reference value. NASA counter-part of peer-reviewed formal professional papers but has less stringent limitations on manuscript length and extent of graphic presentations.

- TECHNICAL MEMORANDUM. Scientific and technical findings that are preliminary or of specialized interest, e.g., quick release reports, working papers, and bibliographies that contain minimal annotation. Does not contain extensive analysis.

- CONTRACTOR REPORT. Scientific and technical findings by NASA-sponsored contractors and grantees.

- CONFERENCE PUBLICATION. Collected papers from scientific and technical conferences, symposia, seminars, or other meetings sponsored or co-sponsored by NASA.

- SPECIAL PUBLICATION. Scientific, technical, or historical information from NASA programs, projects, and missions, often concerned with subjects having substantial public interest.

- TECHNICAL TRANSLATION. English-language translations of foreign scientific and technical material pertinent to NASA's mission.

Specialized services also include organizing and publishing research results, distributing specialized research announcements and feeds, providing information desk and personal search support, and enabling data exchange services.

For more information about the NASA STI program, see the following:

- Access the NASA STI program home page at http://www.sti.nasa.gov

- E-mail your question to help@sti.nasa.gov

- Phone the NASA STI Information Desk at 757-864-9658

- Write to:
  NASA STI Information Desk
  Mail Stop 148
  NASA Langley Research Center
  Hampton, VA 23681-2199

NASA/TM–20230003195

Protective Coatings for Lunar Dust Tolerance

Valerie. L. Wiesner, Christopher J. Wohl, Glen C. King and Keith L. Gordon
Langley Research Center, Hampton, Virginia

Lopamudra Das and Jonathan J. Hernandez
National Institute of Aerospace, Hampton, Virginia

National Aeronautics and
Space Administration

Langley Research Center
Hampton, Virginia 23681-2199

April 2023

Acknowledgments

This work was supported by the Lunar Dust Surface Separation Technology Project under the NASA Space Technology Mission Directorate Game Changing Development Program and the NASA Langley Research Center Innovation Fund and Internal Research and Development Program under the Space Technology Mission Directorate. The authors are grateful to Dr. Kristen John, Erica Montbach, Michael Johansen, Dr. Sharon Miller, Dr. John Connell, Harold Claytor, Dr. Stephen Hales, Dr. David Stegall, Joel Alexa and Dylan Lew for their support of and contribution to this work.

Protective Coatings for Lunar Dust Tolerance

Valerie. L. Wiesner, Christopher J. Wohl, Glen C. King and Keith L. Gordon
Langley Research Center, Hampton, Virginia

Lopamudra Das and Jonathan J. Hernandez
National Institute of Aerospace, Hampton, Virginia

Abstract

Materials capable of withstanding the harsh lunar environment are critically needed to support long duration, sustainable missions on the Moon's surface. Lunar dust significantly threatens the durability and reusability of components and vehicles due to possessing a fine, jagged morphology and highly abrasive nature. These characteristics result in the particles eroding, adhering and/or embedding onto component surfaces and into device confined geometries (e.g., gear housing, interlocking systems, etc.) potentially leading to premature failure. The aim of this study is to identify and characterize wear-resistant commercial-off-the-shelf (COTS) materials, including advanced ceramics, for use as protective coatings to minimize abrasion and adhesion caused by lunar dust. Preliminary testing that mimics various aspects of lunar dust degradation, such as abrasive wear and adhesion, suggests that COTS ceramic coatings can improve lunar dust tolerance and protect underlying metallic substrates.

1. Introduction

Materials resistant to the harsh lunar environment are critically needed to support long duration, sustainable missions on the Moon's surface. Lunar dust poses a significant threat to the durability of components and vehicles due to fine particle size, rough surface morphology and highly abrasive nature of the particles [ref. 1]. These characteristics result in the particles eroding, adhering to and/or embedding on component surfaces and into device confined geometries, potentially leading to premature failure of gear housing, interlocking systems, etc. [ref. 2]. The consensus is that the safety and success of future lunar surface exploration are both dependent on the ability to reduce dust adhesion on, and abrasion of, all exposed equipment.

Numerous lessons were learned from Apollo missions pertaining to lunar dust. The highly refined particles readily adhered to surfaces as a result of mechanical interlocking, chemical bonding and Van der Waals forces, plus electrostatic, Coulombic interactions and donor-acceptor interactions [ref. 3]. Any disturbances of the dust layer at the lunar surface culminated in abrasive wear of exposed surfaces. Pedestrian and vehicular operations, such as sampling/mining activities, caused repeated exposure to dust that resulted in damage accumulation.

Establishing a sustainable presence on the Moon will require a myriad of materials and coating technologies to mitigate the lunar dust problem . Specific components that could be impacted by lunar dust include rover gears, bearings or shafts; lander legs or hatches; habitat joints

or interlocks; and excavating equipment bearings or gears [ref. 4]. For example, a cause of extreme abrasion and wear of lander legs is the rocket plume interactions with the lunar surface that occur during landing and takeoff events. These so-called plume-surface interactions (PSI) can cause dust particulates to be ejected from the lunar surface at velocities upwards of 2,000 m/s resulting in extreme sand blasting of any surfaces in close proximity [ref. 5]. Unfortunately, experimental PSI data from actual Moon landing events are quite sparse. Lunar dust particle velocities and angles of impingement upon lunar landing events by PSI are currently based on theoretical modeling and analyses [refs. 6, 7]. Earth-based PSI testing methods are also limited, which challenges effective evaluation and eventual development of candidate protective materials and technologies for lunar deployment.

Candidate ceramic-based materials may reduce lunar dust adhesion while providing enhanced durability due to superior abrasive and/or erosive wear properties compared with traditional polymeric- and metallic based materials [ref. 8]. In this study, wear-resistant ceramic coatings for application on a reusable lunar lander leg were assessed as part of a NASA-wide effort to enable a sustained lunar presence through the Lunar Surface Innovation Initiative (LSII). A survey of ceramic material systems was performed to identify promising commercially available compositions. Seven coating candidates that could be applied by various processing methods, such as plasma spray, thermal spray and chemical vapor deposition (CVD), while exhibiting adequate mechanical properties, were selected for evaluation [refs. 9, 10]. Ongoing work focuses on testing and validating the efficacy of these materials and coatings in minimizing lunar dust effects. The primary goal is to demonstrate improved performance of a ceramic coating compared to the pristine metal surface of a lander leg fabricated from an aluminum or titanium alloy.

2. Lunar Dust Properties and Considerations

Notable differences between the Moon and Earth are the absence of an atmosphere and that the force of lunar gravity is one-sixth than that of Earth's. Consequently, the lunar surface is exposed to the vacuum of space and bombarded with high-energy radiation. The temperature at the Moon's equator typically ranges from approximately 123°C to -178°C, though it can be even colder at the poles. Furthermore, the much lower gravitational force means that the loose layer of regolith and dust that covers most of the lunar surface is highly mobile.

Lunar regolith is a mix of crystalline and amorphous material, and the composition is location-dependent, similar to Earth. The nominal content comprises 50 wt.% silica (SiO_2), 15 wt.% alumina (Al_2O_3), 10 wt.% calcium oxide (CaO), 10 wt.% magnesium oxide (MgO), 5 wt.% titanium dioxide (TiO_2) and 5–15 wt.% iron with lesser fractions of sodium, potassium, chromium and zirconium compounds [ref. 11]. Traces of nearly all elements can be detected in varying amounts at the parts per million to parts per billion level.

Particle size of lunar dust varies from the nanometer (nm) to millimeter (mm) range with the 1–100 micrometer (µm)-sized particles of primary concern [refs. 12, 13]. A characteristic particle size distribution of µm-sized lunar dust material is highlighted in Figure 1. The lunar dust particles have a nominal density of about 1.5 g/cm^3. The morphology of dust tends to be irregular in shape with a rough surface texture. When coupled with electrostatic charges, particles are reported to readily adhere to moving component and device surfaces [ref. 3].

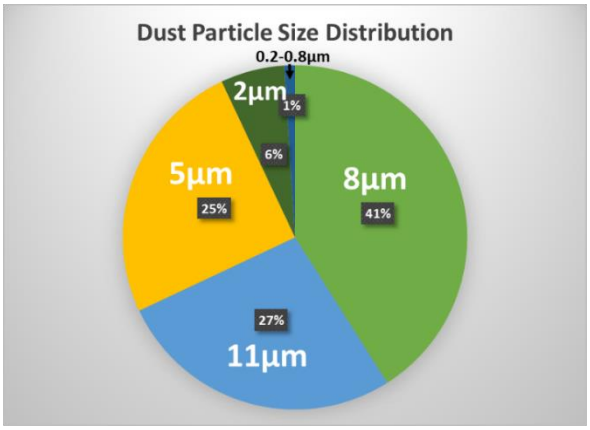

Figure 1 Typical particle size distribution of µm-sized lunar dust.
(Image credit: LaRC)

As highlighted in Figure 2, reported modeling results have indicated that particles can travel anywhere from 20 m to 1000 m from the landing location, assuming nm- to µm-sized lunar dust. Particle velocity estimates range anywhere from 300 m/s to 2000 m/s within 50 m of a landing site depending on particle dimensions, [refs. 5, 7, 14]. These extremely erosive conditions necessitate materials that typically possess exceptional mechanical properties, notably high hardness, such as Vickers hardness (e.g., HV >1000). Thus, advanced ceramics typically used in armor and extreme machining operations become an attractive solution in applications susceptible to wear and abrasion from PSI on the lunar surface.

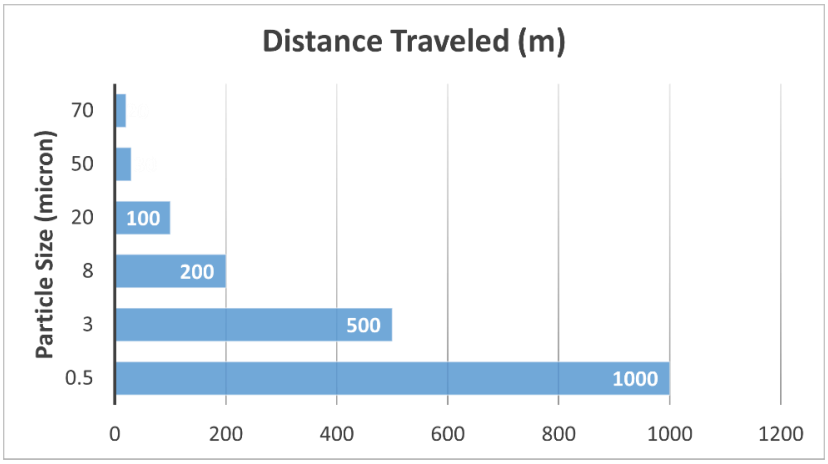

Figure 2 Lunar dust particle size vs. distance traveled from landing site due to plume-surface interaction [data from refs. 5, 7]. (Image credit: LaRC)

3. Selection of Coating Compositions for Lunar Lander Leg Applications

An array of ceramic compositions was assessed for their suitability as coatings on candidate metallic substrates relevant to reusable lunar lander leg structures. The primary considerations that dictated selection of the lunar leg in this study included suitable mechanical properties, which are critical to ensure effective performance. Notably, the component must have appropriate fatigue behavior to withstand multiple landing impacts and takeoff cycles for multiple use. Additionally, the coefficient of thermal expansion (CTE) is another incredibly important consideration such that the material must be able to withstand regular thermal cycling on the Moon's surface. The application and performance of a material that has flown in space also gives important insight into how a material will perform on the lunar surface. As a result, space-heritage materials were considered more flight-proven and preferable over materials without spaceflight demonstration. A literature survey, combined with the GRANTA EduPack©* database package, was utilized to compile relevant material properties, specifically accounting for density, mechanical behavior and processing methods or restrictions.

The substrate materials that were selected for evalution in this work included titanium alloy Ti-6Al-4V and aluminum alloy Al-2219 with pertinent properties shown in Table 1. These alloys were chosen due to their wide utility as aerospace structures, particularly as candidate lunar lander leg materials. Notable differences between the two alloys include that Ti-6Al-4V has a density value that is 1.5 times that of Al-2219, making it less desirable from a weight-savings perspective, while offering a protective benefit of having a hardness three times that of Al-2219.

The commercial-off-the-shelf (COTS) available coating systems that were selected for experimental evaluation included aluminum oxide (alumina, Al_2O_3), aluminum oxide-titanium oxide (alumina-titania, Al_2O_3-TiO_2), boron carbide (B_4C), chromium carbide (Cr_3C_2), chromium carbide-nickel chromium (Cr_3C_2-NiCr), chromium oxide (chromia, Cr_2O_3) and Tribaloy T-800 (a cobalt-chromium-molybdenum (Co-Mo-Cr-Si) alloy). These compositions show promise due to their excellent mechanical properties and success in other aggressive Earth-based applications, such as drilling, mining and protective armor. The relevant material properties, including theoretical density, CTE, processing method average roughness, R_a, and root mean square roughness, R_q, of these candidate coating materials are also given in Table 1.

* Specific vendor and manufacturer names are explicitly mentioned only to accurately describe the hardware used in this study. The use of vendor and manufacturer names does not imply an endorsement by the authors or the U.S. Government nor does it imply that the specified equipment is the best available.

Table 1 Summary of selected properties of substrates and coating compositions evaluated in this study.

Material	Density (g/cm^3)	CTE (µm/m·°C)	Processing Method	R_a (µm)	R_q (µm)
Substrate Materials					
Al-2219	2.84	22.3	-	-	-
Al-6061	2.7	23.6			
Ti-6Al-4V	4.43	9.1	-	-	-
Candidate Coating Material Properties					
Alumina (Al_2O_3)	3.76	8.3	APS	1.43	1.78
Alumina-Titania (Al_2O_3-TiO_2)	3.5	3.9	APS	1.55	1.94
Boron Carbide (B_4C)	2.53	9.4	Vacuum-PS	1.16	1.46
Chromium Carbide (Cr_3C_2)	6.68	10.3	HVOF	0.54	0.68
Chromium Oxide (Cr_2O_3)	5.22	3.7	APS	0.97	1.20
Chromium Carbide-Nickel Chrome (Cr_3C_2-NiCr)	-	6.4	HVOF	0.92	1.17
Co-Mo-Cr-Si (Tribaloy T-800)	8.6	-	HVOF	0.69	0.86

4. Materials and Methods

4.1 Materials and Coating Processing

Each of the COTS coating candidates were applied to Ti-6Al-4V and Al-6061 substrates for the initial phase of this study. Al-6061 was used due to immediate availablity and having properties comparable to Al-2219 (refer to Table 1). Substrates were machined into a series of circular geometries ranging from 1.27 cm to 2.54 cm in diameter. Al_2O_3, B_4C and Cr_3C_2 coatings were deposited by atmospheric plasma spray (APS), vacuum plasma spray and high velocity oxygen fuel (HVOF) methods, respectively, onto the machined substrates (Plasma Processes, Huntsville, AL). Both Al_2O_3-TiO_2 and Cr_2O_3 were applied on the substrates using APS, while Cr_3C_2-NiCr and Co-Mo-Cr-Si coatings were deposited using HVOF (Plasma Technology, Inc., Torrance, CA). Although analysis of coating compositions is underway, this preliminary assessment reports on properties of the notional compositions provided by the supplier. Subsequent work will focus on further characterization of the coating compositions.

4.2 Characterization of Coating Compositions

4.2.1 Mechanical Property and Performance Assessment

A suite of characterization methods to assess the abrasive wear performance and thermal shock resistance of the COTS coatings was performed. A QualTest GT-7012-T Taber Type Abrasion Tester (Taber Industries, North Tonawanda, NY) following ASTM D4060 standard method for abrasion wear was utilized to evaluate the abrasion resistance of the ceramic coatings [ref. 15]. Average coating thickness was determined by collecting three measurements at random locations on the coating surface using a calibrated Eddy current coating thickness gauge instrument (Checkline DCN-3000FX, Lynbrook, NY) to yield an average value for each specimen. Four coated specimens were placed into a custom holder and then simultaneously subjected to a Taber Calibrase CS-17 abrasive wheel (Taber Industries, North Tonawanda, NY) for a set number of cycles. Coating thickness was measured using an Eddy current instrument, along with mass loss, after 400, 1200 and 5000 cycles at 60 Hertz (Hz). Profilometry (FormFactor FRT Microprof 100 profilometer, Livermore, CA) was used before and after abrasion testing to evaluate topography of the coating and wear pattern.

The ability of a coating to withstand thermal shock representative of temperature gradients expected on the lunar surface was evaluated in order to assess material performance issues that could arise due to differences in CTE values between the coating and metallic substrate. Such issues leading to premature coating failure could manifest as coating detachment, spallation and cracking. A single COTS coating specimen was placed into a liquid nitrogen bath, the temperature of which was monitored using a thermocouple, and held for four minutes. This duration was selected to allow sufficient time for the specimen to equilibrate at -194°C, which was the temperature of the liquid nitrogen bath. Then, the specimen was removed from the liquid nitrogen bath and placed on a surface at room temperature. Each specimen was monitored using videography for one to two minutes as it returned to room temperature. After testing, the specimens were examined using optical microscopy.

4.2.2 Surface Roughness and Adhesion Characterization

A FormFactor FRT Microprof 100 profilometer (Livermore, CA) was used for data collection at 10 μm between data points and 40 μm between data lines to assess the surface of the as-deposited COTS coatings. Preliminary roughness parameters, including average roughness, R_a, and root mean square roughness, R_q, were calculated to compare surface roughness across coating compositions and deposition methods and after Taber abrasive wear testing using FormFactor FRT III analysis software. Data was collected in a 2.5 mm by 2.5 mm region on the as-deposited coating surface and then within the Taber abrasive wear path to determine roughness parameters.

The propensity of lunar dust to adhere to the surface of a given coating was measured using a unique, in-house lunar dust sonic wand adhesion screening method (schematic highlighted in Figure 3). The lunar dust adhesion screening method semi-quantitively determines how much lunar dust simulant adheres to a given surface after an exposure. The test involved mounting a coated

specimen using superglue onto a sonic wand tip. Milled lunar dust simulant LHS-1D (Exolith Lab, Oviedo, Florida) with mean particle size of 25 µm was then deposited by an aerosolization technique to the coated specimen surface. Optical micrographs taken before and after the coated specimen was subjected to sonic wand amplitudes were used to assess how much lunar simulant remained on the surface after sonication.

The sonication protocol involved applying 20% of the sonic wand amplitude (maximum displacement for the experimental setup was ~115 µm) at a frequency of 20 kHz for two seconds. This initial sonication step was followed by a 30-second wait period and an additional two seconds at 20% maximum amplitude. This portion of the experimental procedure, hereafter referred to as the cohesion cycle, was implemented to overcome cohesion forces between simulant particles as a way to isolate adhesion interactions between the surface of interest and a simulant particle. Optical images were collected to determine the relative surface coverage of simulant after completion of this step, as some surface adhesion interactions can be comparable to cohesion interactions between simulant particulates. The displacement amplitude was increased from 20% to up to 40% (i.e., ~46 µm) in 5% increments with two second intervals, referred to from here on as the adhesion cycle. The surfaces were imaged again to determine the total simulant clearance from the surface. Particles that came off of the surface could be collected in an optical particle counter located below the instrument as shown in Figure 3.

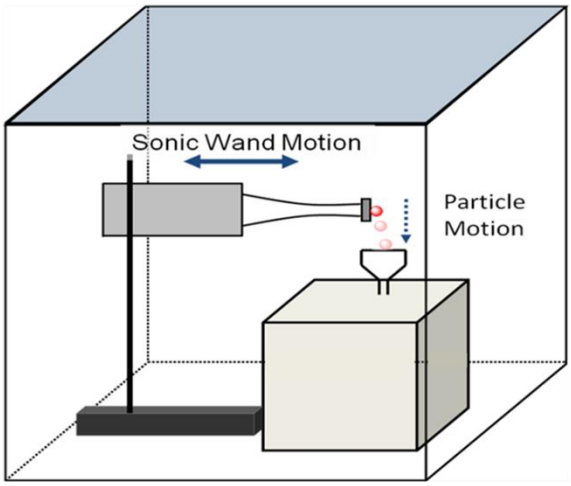

Figure 3 Schematic of lunar dust adhesion test setup. (Image credit: LaRC)

5. Results

5.1 Coating Surface Characterization

The preliminary R_a and R_q values for each coating composition is given in Table 1. Notably, APS Al_2O_3-TiO_2 coatings had the highest R_a and R_q values, implying a higher degree of starting roughness after processing, followed by coatings of Al_2O_3 also processed via APS. Cr_3C_2, Tribaloy T-800 and Cr_3C_2-NiCr coatings deposited by HVOF and Cr_2O_3 by APS, possessed the lowest R_a and R_q values. The surface roughness values measured for all of the coating compositions were comparable to values reported in literature.

5.2 Abrasive Wear Assessment

Abrasive wear results for coatings deposited on Al6061 substrates are shown in Figure 4. Due to minimal weight loss after 5000 cycles across all compositions, weight loss was deemed inconclusive. Consequently, a wear index could not be calculated per ASTM D4060 [ref. 15]. Instead, the change in coating thicknesses between cycles was utilized to assess abrasive wear performance with the least amount of coating loss being most desirable (corresponding to a higher resistance to abrasive wear).

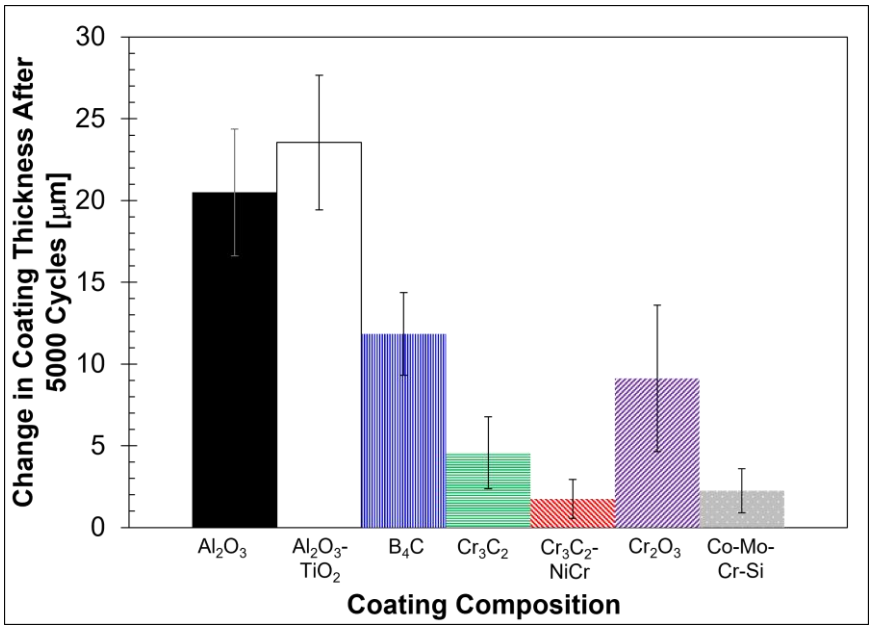

Figure 4 Change in coating thickness after 5000 cycles via Taber abrasive wear testing across all coating compositions.

As presented in Figure 4, changes in coating thickness were observed across all compositions before and after 5000 abrasion cycles. The Al_2O_3-TiO_2 coating exhibited the greatest amount of coating loss with a decrease in coating thickness of over 20 µm after 5000 cycles, suggesting this composition possessed the least resistance to abrasive wear by the Taber method. The most promising coating composition was Cr_3C_2-NiCr, which exhibited the smallest decrease in coating thickness with just under 2 µm after 5000 cycles, followed by both the Tribaloy T-800

and Cr_3C_2 coatings exhibiting overall coating losses of less than 5 µm.

A notable decrease in R_a and R_q values across all compositions was observed by comparing surface roughness of as-processed coatings with surfaces after Taber testing. The percent change in roughness values for each coating composition is plotted in Figure 5. Overall, the Al_2O_3 coating showed the largest decrease in roughness parameters. The Taber wheel track pattern highlighted with dashed lines in the profilometry scan data shown in Figure 6 indicated that the portion of the Al_2O_3 coating in contact with the abrasive wheel was removed during Taber testing. This overall result also seemed to correspond with more significant coating loss as measured by the Eddy current device after Taber testing.

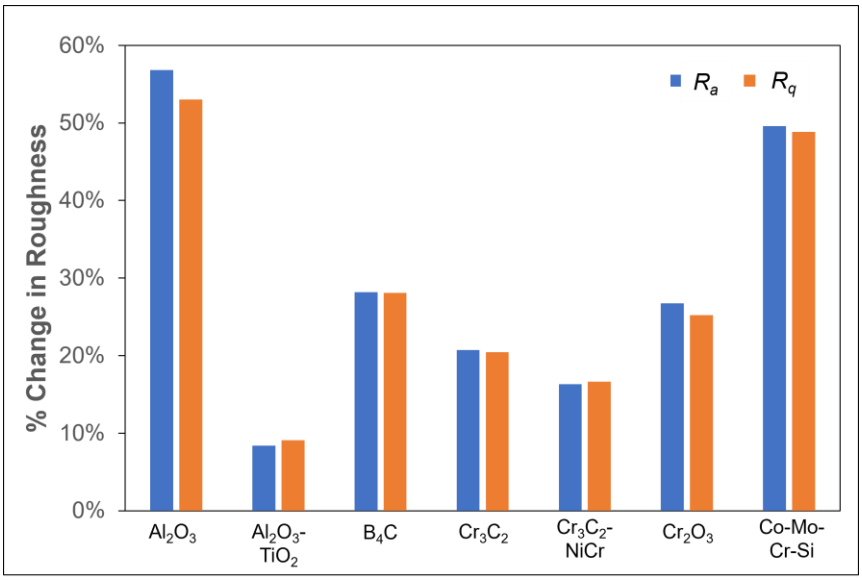

Figure 5 Percent change in roughness R_a and R_q values after 5000 cycles via Taber abrasive wear testing across all compositions.

The compositions that showed minimal coating loss after Taber abrasive wear testing were expected to exhibit the smallest change in roughness parameters. Interestingly, the Tribaloy T-800 coating appeared to lose comparatively little material after Taber testing, yet the percent change in roughness was close to that of the Al_2O_3 coating. This observation was likely a result of the relatively low starting R_a and R_q values of the Tribaloy T-800 coating such that the measured changes of 0.34 µm and 0.42 µm in R_a and R_q, respectively, yielded the second largest percent changes in roughness values. The Al_2O_3-TiO_2 exhibited the smallest relative decrease in roughness values after Taber testing. However, the result for the Al_2O_3-TiO_2 coating showed the highest degree of material loss by Taber abrasion and had the third highest roughness parameters. The next lowest percent changes in roughness were observed in coatings of Cr_3C_2-NiCr, Cr_3C_2, Cr_2O_3 and B_4C as highlighted in Figure 5.

In terrestrial applications that require resistance to abrasive wear, ceramic coatings are typically polished after deposition to achieve an optimal surface finish to yield enhanced abrasive wear performance. Because the coatings in this study were evaluated in the as-received state,

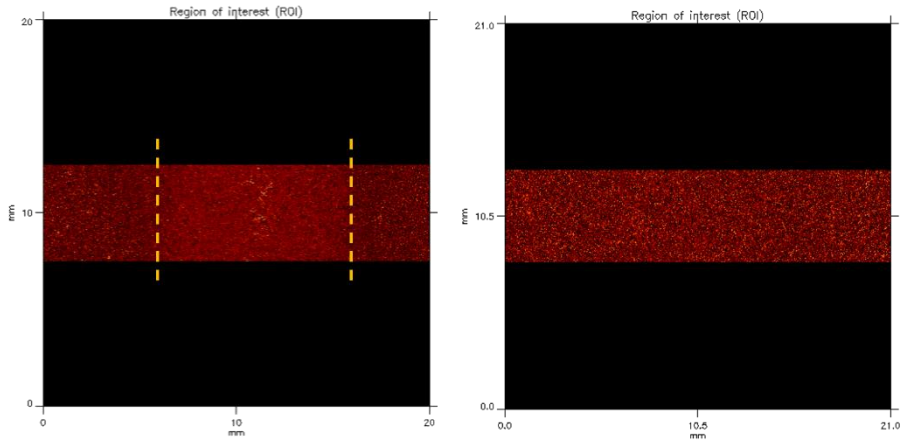

Al_2O_3 Al_2O_3-TiO_2

Figure 6 Profilometry scans of Al_2O_3 and Al_2O_3-TiO_2 coating specimens after Taber testing as labeled. The dashed lines on the Al_2O_3 coating scan highlight the visible track pattern from abrasive wheel after Taber testing, whereas the pattern was not readily detectable on the Al_2O_3-TiO_2 specimen surface.

investigation into the benefits of post-processing polishing for lunar dust tolerant applications will be pursued. Understanding the surface roughness of the coatings is critical to help ascertain the propensity of lunar dust to adhere to a coating barring any abrasive wear or erosive impact. Consequently, further characterization is needed to fully appreciate the mechanisms causing the disparate surface roughness results after Taber abrasive wear testing.

5.3 Sonic Wand Lunar Dust Adhesion Screening

Preliminary data suggested that the COTS coatings have promising dust mitigating properties as deposited. Overall, the optical images of COTS Al_2O_3, Cr_3C_2-NiCr and Tribaloy T-800 coatings showed less dust remaining on surfaces after testing compared with Al_2O_3, B_4C, Cr_3C_2 and Cr_2O_3 coatings. Representative optical microscopy results of the Al_2O_3-TiO_2 and Cr_3C_2-NiCr coatings from before and after dust deposition and after sonication are shown in Figure 7. As shown in Figure 7c and 7f, lesser amounts of dust were observed after sonication than after simulant application, which was a trend observed for all compositions. This observation indicated that dust particles could be effectively removed with sonication, suggesting that the dust particles were less likely to adhere to the coated surfaces. Of the seven COTS compositions, as deposited Al_2O_3, Cr_3C_2-NiCr and Tribaloy T-800 coatings appeared to have moderate dust adhesion mitigating properties, indicating potential as dust adhesion mitigating coatings.

It is important to note that any modifications to surface finish, whether by polishing or even laser ablation patterning, could impact and alter these adhesion results [ref. 16], because the COTS coating specimens were evaluated in the as-deposited state. Consequently, when down-selecting a composition for use in lunar dust tolerant applications, appreciation of the lunar dust adhesion properties on the coating surface will be critical to identify a useful composition. Although the data from the lunar dust sonic wand screening method were semi-quantitative in nature, the data gave a comparative estimate on the ability of lunar dust particles to adhere to a particular surface

relative to other coatings. Further characterization, including profilometry, to more quantitatively assess the amount of lunar simulant dust particles that remains on the surface after deposition and sonication will be utilized.

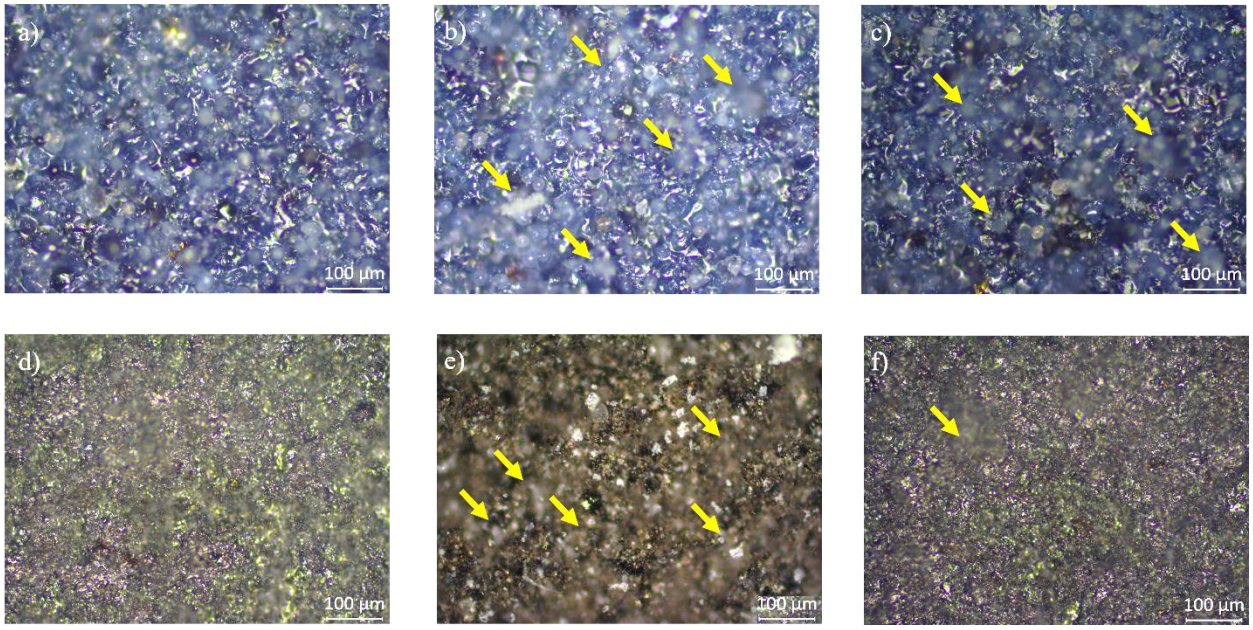

Figure 7 Optical images of coating specimen surfaces of Al_2O_3-TiO_2 (a) before dust deposition, (b) after dust deposition and (c) after sonication and of Cr_3C_2-NiCr (d) before dust deposition, (e) after dust deposition and (f) after sonication. Arrows indicate location of lunar dust simulant particles.

5.4 Thermal Shock Evaluation

Thermocouple monitoring of the liquid nitrogen bath remained consistent at -194°C throughout the test for all seven COTS coatings. Videography of coated specimens upon removal from the liquid nitrogen bath detected no cracking, delamination, spallation or other deleterious failure mode regardless of substrate material. Optical images of the coatings after a minimum of four hours at ambient conditions, shown in Figure 8, also do not reveal any cracking or spallation following the rapid excursion to -194°C. The coatings appeared to possess suitable adhesion to both Al-6061 and Ti-6Al-4V substrates under temperature gradients upwards of 200°C, because the COTS coatings did not delaminate. All seven COTS coating compositions appeared sufficiently adhered irrespective of coating deposition method to both Al-6061 and Ti-6Al-4V substrates despite an order of magnitude difference in CTE values between the COTS coatings and Al-6061 alloy (values shown in Table 1). Further assessments of coating performance under repeated thermal cycling conditions, and at elevated temperatures characteristic of the lunar surface, are underway.

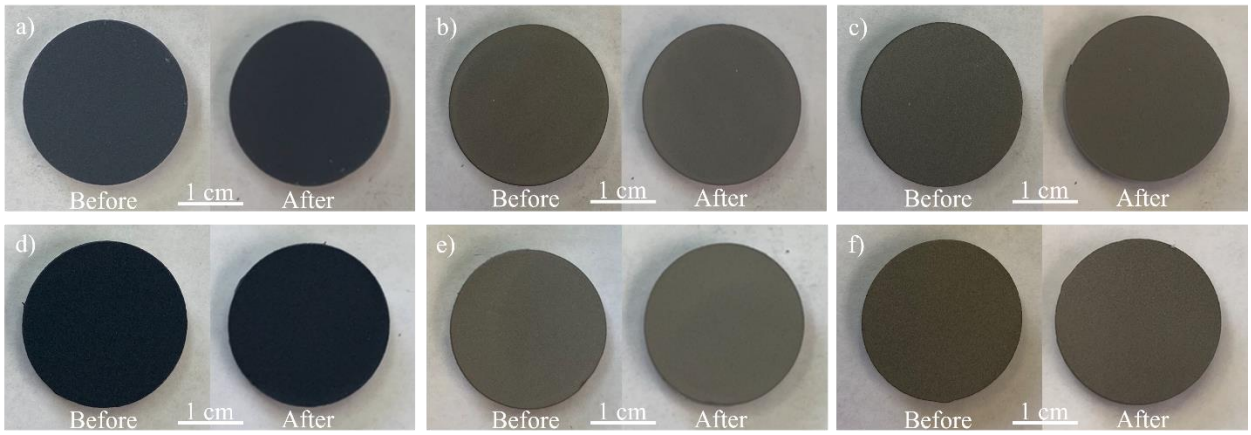

Figure 8 Optical images of (a) Al_2O_3-TiO_2, (b) Cr_3C_2/NiCr and (c) Cr_3C_2 on Al substrates and (d) Al_2O_3-TiO_2, (e) Cr_3C_2/NiCr and (f) Cr_3C_2 on Ti-6Al-4V substrates before and after soak in liquid nitrogen.

6. Summary and Future Work

Materials able to withstand the harsh lunar environment will be critical to the success of long duration missions on the surface of the Moon. Lunar dust threatens the durability of structures and vehicles due to the fine size, irregular morphology and rough surface texture of the particles. The highly abrasive particulates readily erode, adhere to and/or embed in component surfaces, increasing the potential for premature failure. The current effort has identified candidate coating compositions based on COTS materials that could offer protection to lunar components by minimizing the effects of abrasive wear, lunar dust adhesion and thermal gradients >200°C.

The APS Al_2O_3-TiO_2 coatings, with a loss of 23.6 µm ± 4.1 µm in coating thickness after 5000 cycles of Taber abrasion testing, exhibited the lowest wear tolerance of the compositions included in this study. Additionally, lunar dust simulant appeared to more readily adhere to the coating surface in comparison with the other compositions evaluated via the sonic wand lunar dust adhesion screening method. These preliminary results suggested that the as-deposited Al_2O_3-TiO_2 coatings would be undesirable for lunar dust tolerant applications. Conversely, Cr_3C_2-NiCr coatings deposited by HVOF appeared to be the standout coating candidate for lunar dust tolerance based on preliminary results. After 5000 cycles of Taber abrasive wear testing, the Cr_3C_2-NiCr coatings showed the least change in coating thickness with a loss of 1.8 µm ± 1.2 µm. The composition also showed promising lunar dust adhesion performance along with resistance to cracking and delamination due to thermal shock compared with the other coatings. These preliminary findings suggest that Cr_3C_2-NiCr coatings shows significant promise for use in lunar dust tolerant applications.

Further assessment of the microstructure and composition of the COTS materials is underway. Material performance in environments more representative of the lunar surface will also be addressed. The wear behavior of the coatings will be evaluated under vacuum and by particulate erosion. Cr_2O_3, Cr_3C_2 and Cr_3C_2-NiCr compositions, down-selected based on the

findings from this study, will be included on the Materials International Space Station Experiment Flight Facility (MISSE) Mission 16. During the mission, the coatings will be subjected to the low-Earth orbit environment, including solar ultraviolet radiation and atomic oxygen, outside of the International Space Station (ISS). Specimens will be returned and characterized on Earth after the six-month exposure concludes in 2022. The results will allow for selection of coating compositions that will offer benefit to lunar applications, such as reusable lander legs and robust habitat structures, susceptible to damage by lunar dust.

7. References

1. D.S. McKay, G. Heiken, A. Basu, G. Blanford, S. Simon, R. Reedy, B.M. French, J. Papike, "The Lunar Regolith," *Lunar Sourcebook*, Cambridge University Press, 1991, pp. 285-356.
2. T.J. Stubbs, R.R.Vondrak and W.M.Farrell, "Impact of Dust on Lunar Exploration," *Dust in Planetary Systems*, 2007, pp. 239-243.
3. L.H. Lee, "Adhesion and Cohesion Mechanisms of Lunar Dust on the Moon's Surface," *J. Adhesion Sci. Technol*., 1995, 9.8, pp. 1103-1124.
4. M. Hyatt and P. Deluane, "Lunar Dust Mitigation Technology Development," *6th Space Technology and Applications International Forum Session E02-Space Colonization*, 2008, Report E-16717.
5. P.T. Metzger, C.D. Immer, C.M. Donahue, B.T. Vu, R.C. Latta III and M. Deyo-Svendsen, "Jet-induced Cratering of a Granular Surface with Application to Lunar Spaceports," *J. Aerospace Engineering*, 2009, 22.1, pp. 24-32.
6. J.E. Lane, P.T. Metzger, C.D. Immer and X. Li, "Lagrangian Trajectory Modeling of Lunar Dust Particles," *Earth & Space 2008: Engineering, Science, Construction, and Operations in Challenging Environments*, 2008.
7. M.S. Woronowicz, *Modeling of Lunar Dust Contamination Due to Plume Impingement*, Georgia Institute of Technology, 2008.
8. K. Miyoshi, "Solid Lubricants and Coatings for Extreme Environments: State-of-the-Art Survey," 2007, NASA-TM 2007-214668.
9. J.B. Wachtman and R. Haber, *Ceramic Films and Coatings–an Overview*, Noyes Publications, 1993.
10. R. Bunshah and C. Weissmantel, *Handbook of Hard Coatings*, Noyes Publications, 2001.
11. D.J. Loftus, E.M. Tranfield, J.C. Rask and C. McCrossin, *Planetary Science Division Decadal Survey White Paper*, The National Academies Press, 2020.
12. C. Meyer, *NASA Lunar Petrographic Thin Section Set*, NASA JSC Curatorial Branch Publication No. 76, 2003.
13. E. Grün, M. Horanyi, Z. Sternovsky, "The Lunar Dust Environment," *Planetary and Space Science*, 2011, 59, pp. 1672–1680.

14. D. Fontes, J.G. Mantovani, P.T. Metzger, “Numerical Estimations of Lunar Regolith Trajectories and Damage Potential due to Rocket Plumes,” *Acta Astronautica,* 2022, 195, pp. 169-182.
15. ASTM D4060-19, “Test Method for Abrasion Resistance of Organic Coatings by the Taber Abraser,” *ASTM International,* West Conshohocken, PA, 2019.
16. S. Ruiz, Y. Yoo, L. Wadle, X. Chen, N. Li, Y. Lu, C. Wohl, V. Wiesner, B. Cui, “Laser Ablative Patterning of B_4C and MoAlB Ceramics for Hydrophobic Surfaces,” article in review.